



# Silicocarnotite: Novel Silicate Bioceramic With Osteogenic Property for Repairing Rat Cranial Critical-Sized Bone Defects

Yongke Shao<sup>1†</sup>, Fanyan Deng<sup>2†</sup>, Yongyun Chang<sup>3</sup>, Songqing Shi<sup>1</sup>, Huiwu Li<sup>3\*</sup> and Yao Yuan<sup>1\*</sup>

<sup>1</sup>Department of Orthopaedics, Yuyao People's Hospital, Yuyao, China, <sup>2</sup>State Key Laboratory of High Performance Ceramics and Superfine Microstructure, Shanghai Institute of Ceramics, Chinese Academy of Sciences, Shanghai, China, <sup>3</sup>Shanghai Key Laboratory of Orthopaedic Implants, Department of Orthopaedics, Ninth People's Hospital, Shanghai Jiao Tong University School of Medicine, Shanghai, China

## OPEN ACCESS

### Edited by:

Roman Surmenev,  
Tomsk Polytechnic University, Russia

### Reviewed by:

Jiaqiang Liu,  
Shanghai Jiao Tong University, China  
Andre D. R. Silva,  
São Paulo State Technological  
College, Brazil

### \*Correspondence:

Huiwu Li  
huiwu1223@163.com  
Yao Yuan  
395602293@qq.com

<sup>†</sup>These authors have contributed  
equally to this work

### Specialty section:

This article was submitted to  
Biomaterials,  
a section of the journal  
Frontiers in Materials

Received: 13 April 2022

Accepted: 07 June 2022

Published: 15 July 2022

### Citation:

Shao Y, Deng F, Chang Y, Shi S, Li H  
and Yuan Y (2022) Silicocarnotite:  
Novel Silicate Bioceramic With  
Osteogenic Property for Repairing Rat  
Cranial Critical-Sized Bone Defects.  
Front. Mater. 9:919029.  
doi: 10.3389/fmats.2022.919029

Critical-sized bone defects are an intractable orthopedic disease which often fails to regenerate spontaneously and requires additional intervention. Current therapies, including autografts and allografts, are not always satisfactory. Herein, the novel calcium phosphate bioceramic-containing silicon (CPS) with a carnotite structure was synthesized. In the present study, CPS was prepared for investigating the biocompatibility and bioactivity *in vitro* and *in vivo* in comparison to hydroxyapatite (HA). Our results showed that CPS bioceramics had favorable biocompatibility and rBMSCs could adhere on the surface well *in vitro*. Moreover, CPS could promote osteogenic differentiation of rBMSCs and the expression of osteogenic differentiation marker genes, including ALP, Runx-2, BSP, OCN, and OPN. *In vivo*, the results of micro-CT, histomorphometry, and histology analyses showed that CPS significantly enhanced critical-sized calvarial defects healing compared with HA. Overall, the present study demonstrated that CPS bioceramics had satisfactory bioactivities and osteogenic capacities, which could be a potential option for reconstructing critical-sized bone defects.

**Keywords:** silicocarnotite, bioceramic, cytocompatibility, osteogenic differentiation, critical-sized bone defects

## INTRODUCTION

Critical-sized bone defects due to trauma, bone infection, and malignant tumor excision often fail to heal spontaneously in the absence of secondary intervention (Porter et al., 2009; Weng et al., 2018). The reconstruction of critical bone defects is still a major clinical challenge to orthopedic surgeons and usually calls for urgent and efficient handlings (Mehta et al., 2012; Li et al., 2015). Currently, autologous bone grafting is a universal clinical procedure and remains the gold standard in treatment for bone defect repair despite a number of drawbacks (Fillingham and Jacobs, 2016). The sources of autografting are limited by low availability. Furthermore, it could be associated with complications at the donor site and risk of infection, which might prolong hospitalization and increase medical costs

**Abbreviations:** BMD, bone mineral density; CCK-8, cell counting kit-8; CPS, calcium phosphate silicate; HA, hydroxyapatite; H&E, hematoxylin and eosin; rBMSCs, rat bone marrow mesenchymal stem cells;  $\beta$ -TCP,  $\beta$ -tricalcium phosphate; XRD, X-ray diffraction; SEM, scanning electron microscopy.

(Suda et al., 2019). Compared with the autologous bone, allogeneic bone transplantation has many advantages, such as convenient use, relatively abundant sources, low immunogenicity, and can provide structural support. However, the healing of a bone defect is relatively slower in comparison to autografts. Moreover, the enhance risk of infection, transmission, and immunoreactions is a great concern, which limits its clinical applications (Finkemeier, 2002; De Long et al., 2007).

Calcium phosphate ceramics, including hydroxyapatite (HA,  $\text{Ca}_5(\text{PO}_4)_3\text{OH}$ ) and  $\beta$ -tricalcium phosphate ( $\beta$ -TCP,  $\text{Ca}_3(\text{PO}_4)_2$ ), have been widely used in orthopedics as bone graft substitutes, owing to their similar chemical composition to human natural bone tissue and excellent biocompatibility (Tang et al., 2018; Dee et al., 2020). However, they have some disadvantages (Yuan et al., 2010), including limited bioactivities and osteogenic capacities. In addition, the bone's ingrowth is restrained due to the poor degradation rate of these ceramic materials. The aforementioned disadvantages have limited their application in large segmental bone defects. Therefore, it is particularly urgent to find new suitable bone-substitute materials.

Silicon is a vital trace element for bone growth and development. Since Carlisle proposed that silicon was a crucial factor in the calcification of bone tissue in 1970, silicon-based bioceramics and bioglasses have raised considerable attention (Carlisle, 1970). Previous studies have been proved that silicon-containing biomaterials have a good biological activity due to the silicon, which can induce the osteoid apatite matrix formation on the surface of bioceramics in a physiological environment (Motisuke et al., 2017). The properties of silicon-substituted calcium phosphates (Si-HA and Si-TCP) and silica-calcium phosphate composites have been investigated in recent years (Mao et al., 2017). The results of these studies have demonstrated that the addition of silicon can significantly enhance the bioactivity of calcium phosphate bioceramics.

In practice, the calcium phosphate silicate phase [ $\text{Ca}_5(\text{PO}_4)_2\text{SiO}_4$ , CPS] with the silicocarnotite structure is always generated secondarily during the sintering process of silicon-doped calcium phosphate ceramics. However, there are few researches focused on the bioactivity of pure CPS. In order to combine the advantages of calcium phosphate ceramics and the silicon element, a pure CPS biomaterial was synthesized by using a sol-gel method successfully in our present study. The biocompatibility and bioactivity of CPS were comprehensively investigated *in vitro* and *in vivo*.

## MATERIALS AND METHODS

### Preparation of Hydroxyapatite and CPS Scaffolds

HA and CPS powders were synthesized as described previously (Lu et al., 2012). HA powders were prepared by a chemical precipitation method using calcium nitrate tetrahydrate [ $\text{Ca}(\text{NO}_3)_2 \cdot 4\text{H}_2\text{O}$ ] and diammonium phosphate ( $(\text{NH}_4)_2\text{HPO}_4$ ) as the initial materials in an alkaline solution. The precipitates were filtered and washed with deionized water, and dried at 60°C.

Then, the precipitates were sintered at 900°C for 2 h to get HA powders. A sol-gel route was employed to synthesize CPS powders. Tetraethoxysilane (TEOS), triethylphosphate (TEP), and  $\text{Ca}(\text{NO}_3)_2 \cdot 4\text{H}_2\text{O}$  were used as precursors for Si, P, and Ca, respectively. Briefly, TEOS was dropped into a mixture of ethanol and deionized water catalyzing with 2N  $\text{HNO}_3$ . Then, the TEP and  $\text{Ca}(\text{NO}_3)_2 \cdot 4\text{H}_2\text{O}$  were added into the aforementioned solution under stirring to form a uniform solution. The solution was aged at 60°C to form a gel and dried at 120°C. Finally, the dried gel was ground and calcined at 1,350°C for 6 h to produce CPS powders. The obtained HA and CPS powders were uniaxially pressed into disks with a diameter of 5 mm and a thickness of 1 mm and then were sintered at 1,200°C and 1,300°C for 2 h, respectively. Phase composition of the HA and CPS samples were characterized by using the X-ray diffraction method (XRD, D/MAX-RBX, Rigaku, Japan).

### Cell Culture

Rat bone marrow mesenchymal stem cells (rBMSCs) were isolated and expanded as described previously. Rat bone marrow was aspirated from the femoral cavity and was then planted on 10 cm culture dishes in a growth medium consisting of  $\alpha$ -minimal essential medium containing 10% fetal bovine serum, 50 mg/ml streptomycin, and 50 U/ml penicillin. The dishes were incubated in an incubator at the atmospheric temperature of 37°C and 5%  $\text{CO}_2$ . rBMSCs between the third and fifth passages were applied in our study. For the experiments, rBMSCs were cultured in an osteogenic medium consisting of the growth medium with the addition of 100 nM dexamethasone, 10 mM  $\beta$ -glycerophosphate, and 50  $\mu\text{M}$  ascorbic acid.

### Scanning Electron Microscopy Analysis of Cell Morphology

The cells on the surface of disks were washed with pre-cooling PBS thrice and fixed with 2.5% glutaraldehyde for 1 h at 4°C. Then, the cells were dehydrated in a graded series of ethanol with different concentration gradients (30%, 50%, 70%, 90%, 95%, and 100%) for 15 min each. The samples were air-dried overnight and then sprayed with powdered gold for SEM examination. The cellular morphology was observed by SEM (SEM450, FEI Nova Nano SEM; Thermo Fisher Scientific, Waltham, MA, United States).

### Cell Proliferation Assay

RBMSCs were seeded on the surface of the disks at a density of 3,000 cells/cm<sup>2</sup>. A cell counting kit-8 (CCK8) assay (Dojindo, Kumamoto, Japan) was used to assess the cell viability and proliferation at 24, 48, and 72 h. The cells-seeded disks were incubated in a basic medium containing 10% CCK8 solution for 2 h at an atmospheric temperature of 37°C and 5%  $\text{CO}_2$ . The Multi-scan UV-visible spectrophotometer (Safire2; TECAN, Mannedorf, Switzerland) was applied to measure the absorbance at 450 nm.

### ALP Staining

RBMSCs were seeded onto HA and CPS disks and cultured at 37°C and 5%  $\text{CO}_2$ . After 24 h of cell attachment, the medium with

**TABLE 1** | Primer sequences for real-time PCR.

Gene	Forward (5'-3')	Reverse (5'-3')
rat-ALP	GACAATGAGATGCCGCCAGAG	CATCCAGTTCATATTCCACATCAGTTC
rat-Runx2	ACTATCCAGCCACCTTCACCTTACA	TCAGCGTCAACACCATCATTCT
rat-BSP	CACTGCGTATGAAACCTAT	GTAGTAATAATCCTGACCCTC
rat-OCN	GGACCCTCTCTGCTCACTCTG	ACCTTACTGCCCTCCTGCTTGG
rat-OPN	CAGTATCCCGATGCCACA	CAGTATCCCGATGCCACA
rat-GAPDH	GCAAGTTCAACGGCACAG	GCCAGTAGACTCCACGACAT

osteogenic supplements was used to substitute the growth culture medium. The medium was changed every 2 days. After 7 days of culture, the activity of alkaline phosphatase (ALP) was detected with an ALP kit (Beyotime, Jiangsu, China) according to the manufacturer's instructions.

### Real-Time RT-PCR

Total RNA was extracted from attached cells using the TRIzol reagent (Invitrogen, Carlsbad, CA, United States). The RNA concentration was measured with a micro-spectrophotometer at 260 nm. RNA was reverse-transcribed into cDNA with a PrimeScript RT Master Mix kit (Takara, Shiga, Japan). The obtained reaction solution was used to perform the next Real-time PCR reaction with SYBR Premix Ex Taq (Takara, Shiga, Japan). The housekeeping gene GAPDH was employed as an internal control. Data of different target genes were analyzed with the comparison Ct ( $2^{-\Delta\Delta C_t}$ ) method and expressed as fold changes compared to the GAPDH expression. Primer sequences of each gene are listed in **Table 1**.

### Animals and Surgical Procedure

Animal experiments were conducted with the permission of the Animal Care and Experimentation Ethics Committee of Shanghai Ninth People's Hospital, Shanghai Jiao Tong University School of Medicine. The animals were raised in a specified pathogen-free (SPF) environment. A total of nine 12-week-old male Sprague-Dawley rats (weight: 300–350 g each) were randomly divided into three groups: 1) Blank, 2) HA, and 3) CPS. Prefabricated scaffolds ( $n = 6$ ) with the same method as previously described were prepared for each group. Briefly, the rats were anesthetized *via* intraperitoneal injection using 1.0% sodium pentobarbital (100 mg/kg). Then, the hair of the surgical area was shaved and disinfected. A 1.5 cm sagittal incision was made on the scalp and the skull was exposed carefully. After exposing the calvarium, a symmetric circular bone defect of 5 mm in diameter was made via a trephine bur on both sides of the head. HA and CPS ceramic scaffolds were implanted. The subcutaneous fascia and skin were sutured by layer. The rats were sacrificed at 8 weeks post-operation, and the skulls were harvested for subsequent processes.

### Micro-Computed Tomography Measurement

To analyze new bone formation after implantation, the scaffolds with the surrounding calvarial bone were extracted out and

analyzed using a micro-CT imaging system (skyscan 1072; Skyscan, Aartselaar, Belgium). Briefly, the rat calvariums were collected and fixed in 4% paraformaldehyde. Subsequently, the specimens were scanned with a voltage of 70 kV, current of 114  $\mu$ A, and a resolution of 10  $\mu$ m per pixel. Finally, three-dimensional (3D) images in bone defects were reconstructed and microstructure indexes were analyzed, including the bone mineral density (BMD,  $1/\text{mm}^3$ ), bone volume/total tissue volume (BV/TV, %), trabecular thickness (Tb.Th, mm), and trabecular number (Tb.N,  $1/\text{mm}$ ).

### Histopathological Analysis

Following the micro-CT scan, the retrieved cranial specimens were soaked in 10% EDTA decalcifying solution (pH = 7.4) for 21 days. After decalcification, the samples were dehydrated through an increasing graded series of ethanol and then embedded in paraffin. Multiple 5  $\mu$ m thick sections were performed and stained with hematoxylin and eosin (H&E), Masson-trichrome staining in accordance with the manufacturer's protocols (Servicebio Technology Co., Ltd., Wuhan, China). The images were obtained using a microscope.

### Statistical Analysis

Data are presented as the mean  $\pm$  standard deviation (SD). A statistical analysis was performed by using the Student's t test between two groups and one-way analysis of variance followed by Student-Newman-Keuls post-hoc test between three or more groups.  $p$  value  $<0.05$  was considered statistically significant.

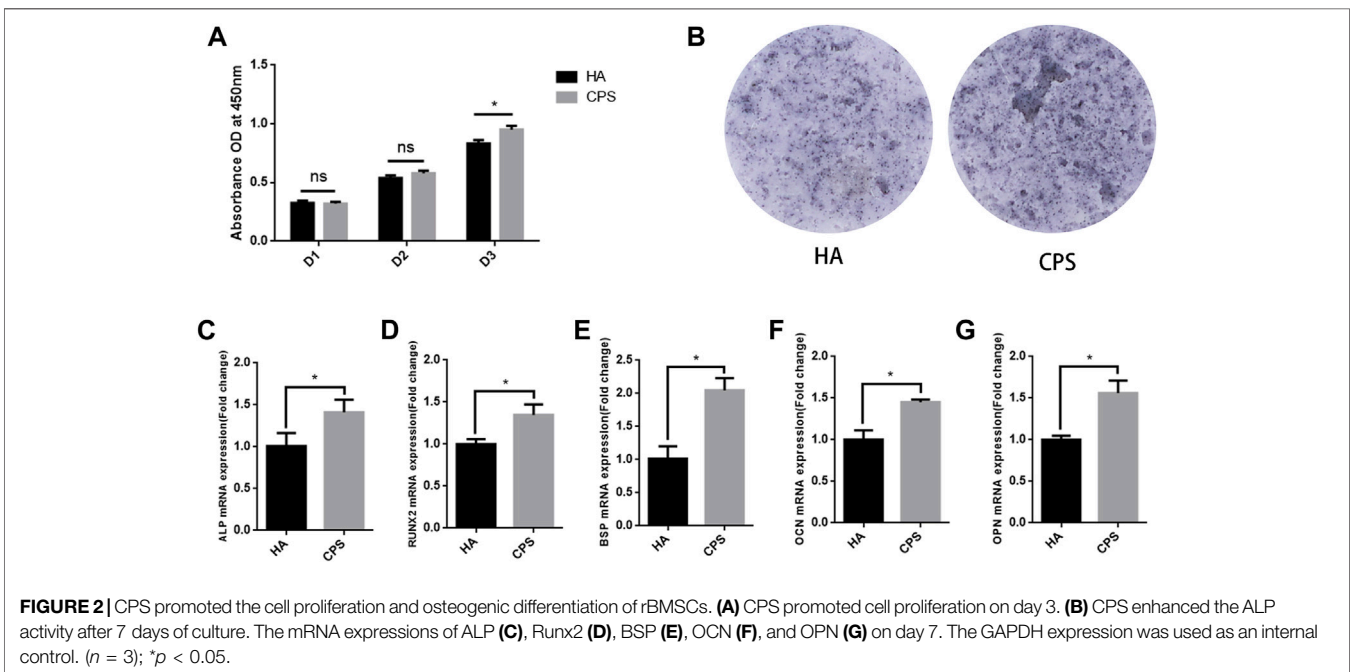
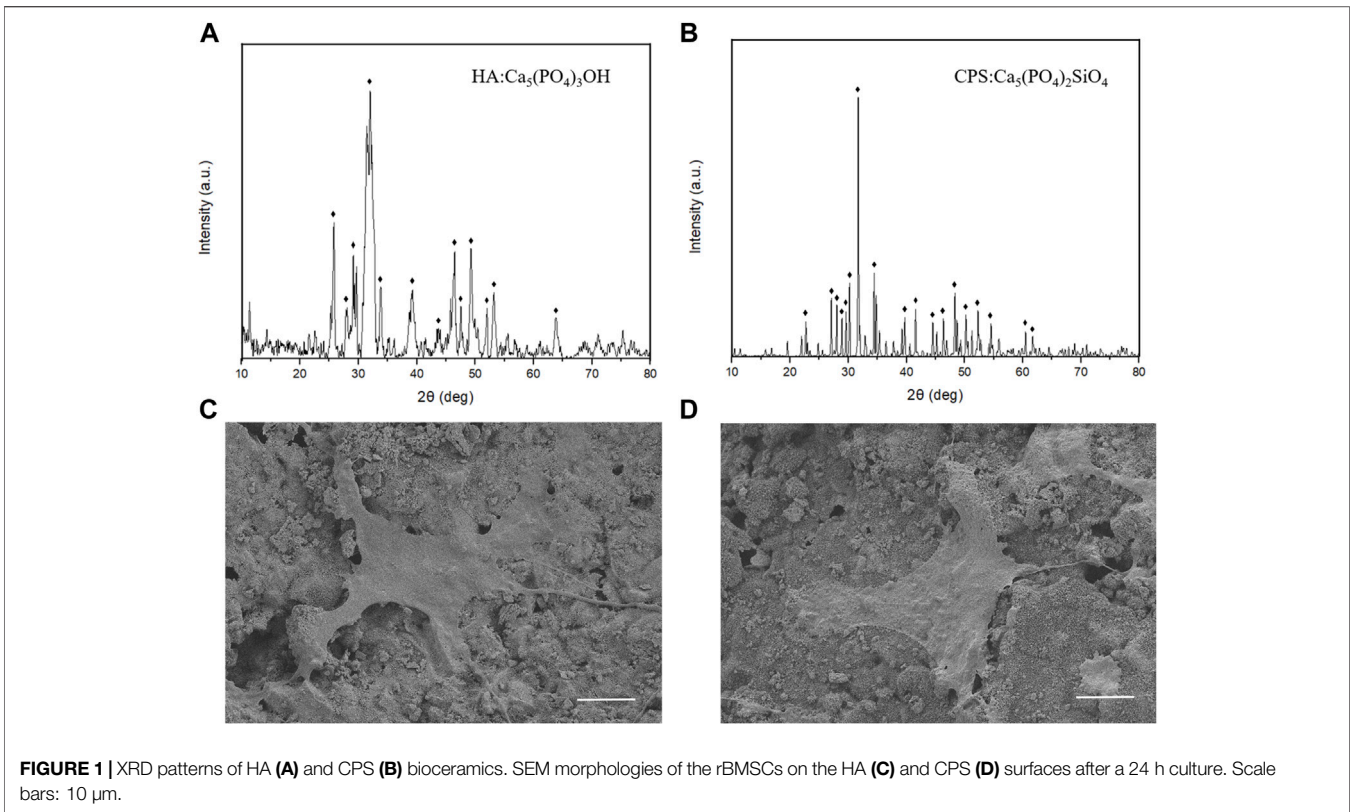
## RESULTS

### Characterization of Hydroxyapatite and CPS Bioceramics

The XRD patterns of the prepared ceramics of HA and CPS are shown in **Figures 1A,B**, respectively. The XRD patterns of HA and CPS coincided well with the standard  $\text{Ca}_5(\text{PO}_4)_3\text{OH}$  PDF card (JCPDS card: No 09-0432) and  $\text{Ca}_5(\text{PO}_4)_2\text{SiO}_4$  PDF card (JCPDS card: No 40-0393). These results indicated that pure HA and CPS ceramics were made.

### Morphology of rBMSCs on Hydroxyapatite and CPS

To evaluate the morphology of rBMSCs on HA and CPS bioceramic disks, SEM was applied. The SEM images showed



that the shapes of rBMSCs had no significant differences between the two groups (Figures 1C,D). Both of them spread well, and a large number of prominent filopodia and lamellipodia could be

noticeably observed. These results revealed that the HA and CPS bioceramics had good biocompatibility and rBMSCs could adhere on the surface well.

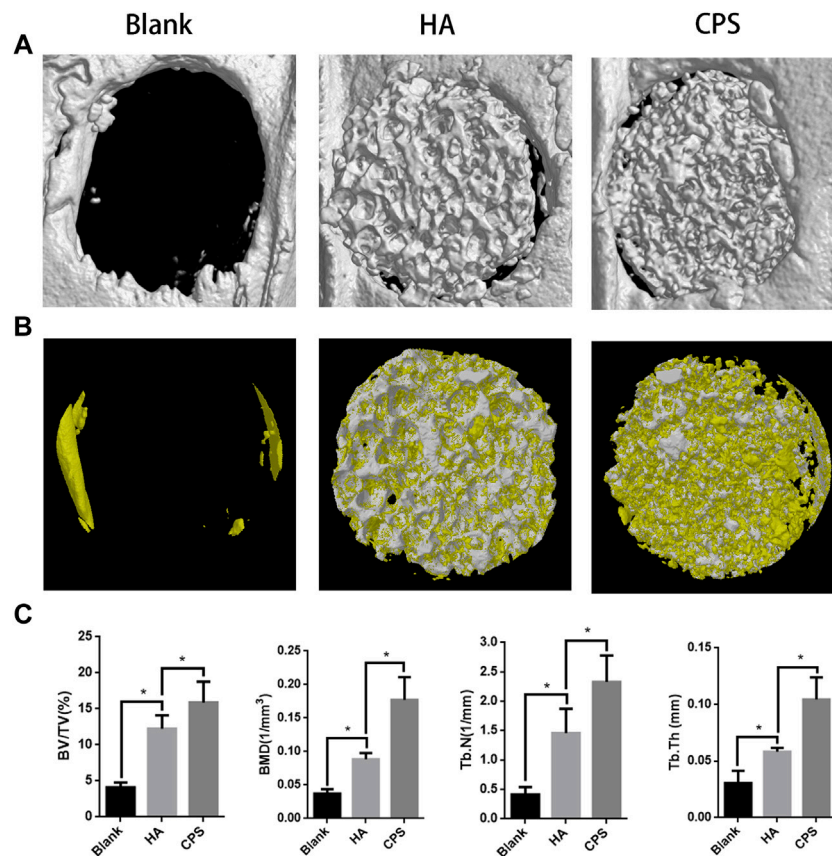


**FIGURE 3** | Micro-CT analysis of the osteogenic property within bone defects *in vivo*. **(A)** Micro-CT images of the repaired skull after 8 weeks of implantation. **(B)** 3D-reconstruction images of Micro-CT. The yellow part represents the new bone, and the white represents the scaffold. **(C)** A morphometric analysis of micro-CT, including BV/TV, BMD, Tb.N, and Tb.Th. \* $p < 0.05$ .

### Cell Proliferation of rBMSCs on Hydroxyapatite and CPS

To investigate the proliferation of rBMSCs on HA and CPS, we conducted CCK8 assays with the increase of culture time. Our results showed that the cell proliferation rate on the surface of CPS was higher than that on HA after 72 h of incubation; however, there were no significant differences in cell numbers after 24 and 48 h between the two groups (Figure 2A).

### CPS Promoted the Osteogenic Property of rBMSCs *In Vitro*

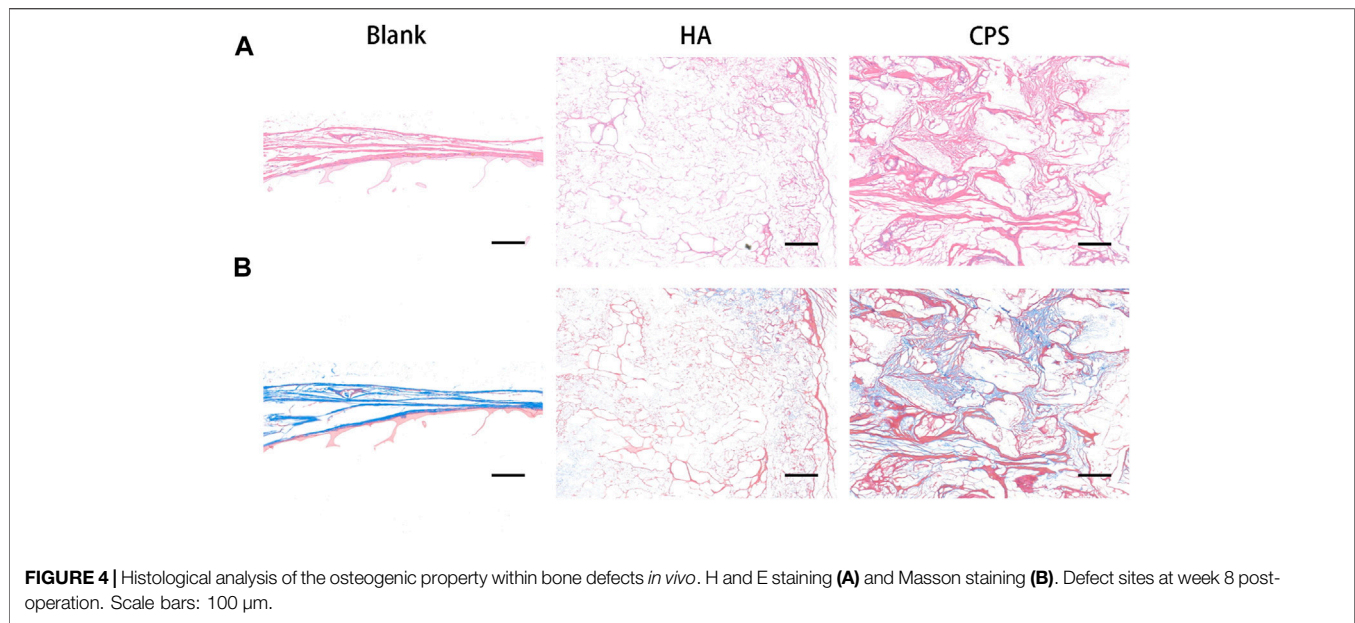
To evaluate the osteogenic properties of HA and CPS *in vitro*, we performed ALP staining and qRT-PCR assays. The results of ALP staining demonstrated that the level of ALP activities in the CPS group was significantly higher than that in HA group after osteogenic induction for 7 days (Figure 2B). In the PCR analysis, the expression of the osteogenic differentiation-related marker genes including ALP, Runx2, BSP, OCN, and OPN in the CPS group were significantly increased at day 7 in comparison to the HA group (Figures 2C–G).

### CPS Scaffold Enhanced Osteogenic Property *In Vivo*: Micro-Computed Tomography Analysis

Micro-CT was applied to assess the osteogenic property of HA and CPS scaffolds *in vivo*. The images of the micro-CT revealed that more new bone calluses formed in the CPS groups in comparison to those in the HA group at 8 weeks post-operation (Figure 3A). The 3D-reconstructed images demonstrated that more new bones ingrowth and achieved more new bone colonization in the CPS scaffolds compared to the HA scaffold at 8 weeks after surgery (Figure 3B). A histomorphometry analysis of the callus tissue showed that the values of BMD, BV/TV, Tb.N, and Tb.Th were significantly increased in the CPS group than that in the HA group (Figure 3C).

### CPS Scaffold Enhanced Osteogenic Property *In Vivo*: Histological Analysis

A histological analysis was carried out to assess the osseointegration property of the HA and CPS scaffolds at 8 weeks post-operation. H&E and Masson staining were



conducted to assess the healing of cranial bone defects in the bone sections. In H&E staining (Figure 4A), the CPS group had less residual scaffolds and more new bone calluses than the HA scaffold. However, the defect was mainly occupied by fibrous tissues in the HA group at 8 weeks post-operation. In Masson staining (Figure 4B), compared with the HA group, more new bones were found inside the scaffolds in the CPS groups. These results indicated that CPS had a better osteogenic property than HA.

## DISCUSSION

Critical-sized bone defects are often caused by trauma, skeletal diseases, tumor resections, and other orthopedic surgeries. Currently, more than four million graft surgeries are conducted each year to deal with these bone defects, which makes bone the second most commonly transplanted tissue worldwide (Turnbull et al., 2018). However, the reconstruction of bone defects remains a great challenge in orthopedics and usually requires urgent and effective disposing, restoring the mechanical and biological functions of the bone (Song et al., 2017). Autografts are currently the most commonly used treatment of bone defects and are still the clinical gold standard. However, they also suffer from limited sources, a secondary surgical site, and donor area complications including infection and pain. On the other hand, allografts enhanced the risk of infectious transmission and immune response. The prevalence of bone defects, their relevant morbidity, and high socio-economic cost necessitates the need for new bone substitute materials to promote the bone defects' repair and regeneration (Black et al., 2015; Parmentier et al., 2020).

In recent years, calcium phosphate bioceramics have become one of the most popular bone mimic substitutes because of their

fine biocompatibility and osteo-conductivity, including HA and  $\beta$ -TCP (Tsukanaka et al., 2015; Liu et al., 2016). However, HA has a poor degradation rate and high fragility that may cause broken implants and hard handling characteristics. In addition,  $\beta$ -TCP has low strength and poor mechanical properties. Therefore, in order to meet the growing demand for bone defect grafts, it is particularly urgent to find suitable new bioceramic materials. Silicon is an indispensable trace element for bone growth and development. Hence, silicon-containing bioglasses and bioceramics as bone substitute materials have attracted much attention (Ning et al., 2004; Bohner, 2009). Studies have been proved that Si-containing glasses and bioceramics were highly bioactive and could stimulate cellular biological activities, for instance, cell proliferation and osteogenic differentiation. The bioactivity improvement of Si-substituted materials can be ascribed to a number of factors that act synergistically (Manchón et al., 2015). Si-substitution facilitates protein adsorption and osteoblasts' attachment and proliferation. Si, which is released to the extracellular matrix or presented in the implant surface, has a direct effect on osteoblasts, osteoclasts, and collagen synthesis. CPS, a novel silicon-containing calcium phosphate bioceramic with a carnotite structure, has great potential as a bone graft material. In our study, the cytocompatibility and osteogenic differentiation activity of CPS were investigated thoroughly *in vitro* and *in vivo*.

Good biocompatibility is the basic requirement for bone substitute materials. *In vitro*, the rBMSCs grew and spread well on CPS disks and the filopodia and lamellipodia could be noticeably observed, which suggested that CPS had a favorable biocompatibility. In addition, the results of the CCK-8 assay showed that the proliferation rate of rBMSCs on the CPS surface was significantly higher than that on the surface of HA after 72 h culture, implying that CPS could enhance cell proliferation. Osteogenic differentiation is one of the vital processes for bone regeneration. The results of ALP staining and qRT-PCR

experiments showed that CPS possessed a better property to promote osteogenic differentiation of rBMSCs than HA. Previous studies have demonstrated that Si in aqueous solutions could promote osteoblast proliferation and enhance alkaline phosphatase activity and the expression of osteocalcin. In addition, CPS can induce bone-like apatite formations in simulated body fluids (SBFs) in a short time (Lu et al., 2012). CPS could also adsorb more amount and types of serum proteins than HA, including FN1 and IGF1. A pathway analysis revealed that these absorbed proteins by CPS helped mediate cell adhesion and promoted osteogenic activity, which might indicate a better osteogenic potential of CPS (Deng et al., 2021). In our study, the detailed mechanisms of the enhancement of cell proliferation and osteogenic differentiation needed to be further studied.

*In vivo*, the results of the micro-CT and histological analysis did further prove that CPS scaffolds had significant accelerative effects for bone defect restoration in a rat's cranial critical-sized bone defect model. The ideal bone regenerative material should have good biocompatibility, osteoconductivity, and osteoinductivity (Yu et al., 2015). In our study, the results of the micro-CT showed that CPS scaffolds had more new bone ingrowth than the HA scaffold. The histomorphometry analysis of the new bone callus tissue also showed that the values of BMD, BV/TV, Tb.Th, and Tb.N were significantly increased in the CPS group than that in the HA group. On the other hand, the histological analysis of H and E and Masson staining had similar trends. Compared with the HA group, more new bones and less fibrous residual scaffolds were found in the CPS groups. Hing et al. (2006) has shown that the porous silicate-substituted hydroxyapatite increased bone deposition and ingrowth in a femoral intercondylar defect in New Zealand white rabbits. Similar results were obtained by Patel et al. (2002). They implanted pure HA and Si-substituted HA granules in a rabbit model, and observed that the bone ingrowth and bone-implant coverage were significantly greater in Si-HA than that in pure HA. In our study, CPS

improved new bone formation in a rat skull defect model, which was consistent with previous findings.

Our study showed that CPS exhibited fine bioactivities and osteogenic capacities in treating critical-sized bone defects. *In vitro*, CPS had a good cell adhesion behavior and increased cell proliferation and osteogenesis. *In vivo*, CPS presented good bioactivities, degradability, and bone ingrowth properties. All the data indicated that CPS could be a promising candidate for the reconstruction of critical-sized bone defects.

## DATA AVAILABILITY STATEMENT

The original contributions presented in the study are included in the article/Supplementary Material; further inquiries can be directed to the corresponding authors.

## ETHICS STATEMENT

The animal study was reviewed and approved by the Animal Care and Experimentation Ethics Committee of Ninth People's Hospital, Shanghai Jiao Tong University School of Medicine.

## AUTHOR CONTRIBUTIONS

Conception and design: HL and YY; conducting the *in vitro* and *in vivo* experiments: YS and FD; collection and assembly of data: YC and SS; data analysis and interpretation: YS and FD; manuscript writing and final approval of manuscript: all authors.

## FUNDING

This work was supported by the Ningbo Medical Science and Technology Project (Grant No. 2017A37).

## REFERENCES

- Black, C. R. M., Goriainov, V., Gibbs, D., Kanczler, J., Tare, R. S., and Oreffo, R. O. C. (2015). Bone Tissue Engineering. *Curr. Mol. Bio Rep.* 1 (3), 132–140. doi:10.1007/s40610-015-0022-2
- Bohner, M. (2009). Silicon-substituted Calcium Phosphates - a Critical View. *Biomaterials* 30 (32), 6403–6406. doi:10.1016/j.biomaterials.2009.08.007
- Carlisle, E. M. (1970). Silicon: a Possible Factor in Bone Calcification. *Science* 167 (3916), 279–280. doi:10.1126/science.167.3916.279
- De Long, W. G., Jr., Einhorn, T. A., Koval, K., McKee, M., Smith, W., Sanders, R., et al. (2007). Bone Grafts and Bone Graft Substitutes in Orthopaedic Trauma Surgery. *J. Bone & Jt. Surg.* 89 (3), 649–658. doi:10.2106/jbjs.f.00465
- Dee, P., You, H. Y., Teoh, S.-H., and Le Ferrand, H. (2020). Bioinspired Approaches to Toughen Calcium Phosphate-Based Ceramics for Bone Repair. *J. Mech. Behav. Biomed. Mater.* 112, 104078. doi:10.1016/j.jmbbm.2020.104078
- Deng, F., Zhai, W., Yin, Y., Peng, C., and Ning, C. (2021). Advanced Protein Adsorption Properties of a Novel Silicate-Based Bioceramic: A Proteomic Analysis. *Bioact. Mater.* 6 (1), 208–218. doi:10.1016/j.bioactmat.2020.08.011
- Fillingham, Y., and Jacobs, J. (2016). Bone Grafts and Their Substitutes. *Bone & Jt. J.* 98-b (1), 6–9. doi:10.1302/0301-620x.98b.36350
- Finkemeier, C. G. (2002). Bone-grafting and Bone-Graft Substitutes. *J. Bone Jt. Surgery-American Volume* 84 (3), 454–464. doi:10.2106/00004623-200203000-00020
- Hing, K. A., Revell, P. A., Smith, N., and Buckland, T. (2006). Effect of Silicon Level on Rate, Quality and Progression of Bone Healing within Silicate-Substituted Porous Hydroxyapatite Scaffolds. *Biomaterials* 27 (29), 5014–5026. doi:10.1016/j.biomaterials.2006.05.039
- Li, L., Zhou, G., Wang, Y., Yang, G., Ding, S., and Zhou, S. (2015). Controlled Dual Delivery of BMP-2 and Dexamethasone by Nanoparticle-Embedded Electrospun Nanofibers for the Efficient Repair of Critical-Sized Rat Calvarial Defect. *Biomaterials* 37, 218–229. doi:10.1016/j.biomaterials.2014.10.015
- Liu, X., Bao, C., Xu, H. H. K., Pan, J., Hu, J., Wang, P., et al. (2016). Osteoprotegerin Gene-Modified BMSCs with Hydroxyapatite Scaffold for Treating Critical-Sized Mandibular Defects in Ovariectomized Osteoporotic Rats. *Acta Biomater.* 42, 378–388. doi:10.1016/j.actbio.2016.06.019
- Lu, W., Duan, W., Guo, Y., and Ning, C. (2012). Mechanical Properties and *In Vitro* Bioactivity of Ca<sub>5</sub>(PO<sub>4</sub>)<sub>2</sub>SiO<sub>4</sub> Bioceramic. *J. Biomater. Appl.* 26 (6), 637–650. doi:10.1177/0885328210383599
- Manchón, A., Alkhraisat, M., Rueda-Rodríguez, C., Torres, J., Prados-Frutos, J. C., Ewald, A., et al. (2015). Silicon Calcium Phosphate Ceramic as Novel

- Biomaterial to Simulate the Bone Regenerative Properties of Autologous Bone. *J. Biomed. Mat. Res.* 103 (2), 479–488. doi:10.1002/jbm.a.35196
- Mao, L., Xia, L., Chang, J., Liu, J., Jiang, L., Wu, C., et al. (2017). The Synergistic Effects of Sr and Si Bioactive Ions on Osteogenesis, Osteoclastogenesis and Angiogenesis for Osteoporotic Bone Regeneration. *Acta Biomater.* 61, 217–232. doi:10.1016/j.actbio.2017.08.015
- Mehta, M., Schmidt-Bleek, K., Duda, G. N., and Mooney, D. J. (2012). Biomaterial Delivery of Morphogens to Mimic the Natural Healing Cascade in Bone. *Adv. Drug Deliv. Rev.* 64 (12), 1257–1276. doi:10.1016/j.addr.2012.05.006
- Ming, C. Q., Greish, Y., and El-Ghannam, A. (2004). Crystallization Behavior of Silica-Calcium Phosphate Biocomposites: XRD and FTIR Studies. *J. Mater. Sci. Mater. Med.* 15 (11), 1227–1235. doi:10.1007/s10856-004-5677-9
- Motisque, M., Mestres, G., Renó, C. O., Carrodeguas, R. G., Zavaglia, C. A. C., and Ginebra, M.-P. (2017). Influence of Si Substitution on the Reactivity of  $\alpha$ -tricalcium Phosphate. *Mater. Sci. Eng. C* 75, 816–821. doi:10.1016/j.msec.2017.02.099
- Parmentier, L., Riffault, M., and Hoey, D. A. (2020). Utilizing Osteocyte Derived Factors to Enhance Cell Viability and Osteogenic Matrix Deposition within IPN Hydrogels. *Materials* 13 (7), 1690. doi:10.3390/ma13071690
- Patel, N., Best, S. M., Bonfield, W., Gibson, I. R., Hing, K. A., Damien, E., et al. (2002). A Comparative Study on the *In Vivo* Behavior of Hydroxyapatite and Silicon Substituted Hydroxyapatite Granules. *J. Mater. Sci. Mater. Med.* 13 (12), 1199–1206. doi:10.1023/a:1021114710076
- Porter, J. R., Ruckh, T. T., and Popat, K. C. (2009). Bone Tissue Engineering: a Review in Bone Biomimetics and Drug Delivery Strategies. *Biotechnol. Prog.* 25 (6), NA. doi:10.1002/btpr.246
- Song, F., Sun, H., Huang, L., Fu, D., and Huang, C. (2017). The Role of Pannexin3-Modified Human Dental Pulp-Derived Mesenchymal Stromal Cells in Repairing Rat Cranial Critical-Sized Bone Defects. *Cell Physiol. Biochem.* 44 (6), 2174–2188. doi:10.1159/000486023
- Suda, A. J., Schamberger, C. T., and Viergutz, T. (2019). Donor Site Complications Following Anterior Iliac Crest Bone Graft for Treatment of Distal Radius Fractures. *Arch. Orthop. Trauma Surg.* 139 (3), 423–428. doi:10.1007/s00402-018-3098-3
- Tang, Z., Li, X., Tan, Y., Fan, H., and Zhang, X. (2018). The Material and Biological Characteristics of Osteoinductive Calcium Phosphate Ceramics. *Regen. Biomater.* 5 (1), 43–59. doi:10.1093/rb/rbx024
- Tsukanaka, M., Fujibayashi, S., Otsuki, B., Takemoto, M., and Matsuda, S. (2015). Osteoinductive Potential of Highly Purified Porous  $\beta$ -TCP in Mice. *J. Mater. Sci. Mater. Med.* 26 (3), 132. doi:10.1007/s10856-015-5469-4
- Turnbull, G., Clarke, J., Picard, F., Riches, P., Jia, L., Han, F., et al. (2018). 3D Bioactive Composite Scaffolds for Bone Tissue Engineering. *Bioact. Mater.* 3 (3), 278–314. doi:10.1016/j.bioactmat.2017.10.001
- Weng, L., Boda, S. K., Wang, H., Teusink, M. J., Shuler, F. D., and Xie, J. (2018). Novel 3D Hybrid Nanofiber Aerogels Coupled with BMP-2 Peptides for Cranial Bone Regeneration. *Adv. Healthc. Mat.* 7 (10), 1701415. doi:10.1002/adhm.201701415
- Yu, X., Tang, X., Gohil, S. V., and Laurencin, C. T. (2015). Biomaterials for Bone Regenerative Engineering. *Adv. Healthc. Mat.* 4 (9), 1268–1285. doi:10.1002/adhm.201400760
- Yuan, H., Fernandes, H., Habibovic, P., de Boer, J., Barradas, A. M. C., de Ruiter, A., et al. (2010). Osteoinductive Ceramics as a Synthetic Alternative to Autologous Bone Grafting. *Proc. Natl. Acad. Sci. U.S.A.* 107 (31), 13614–13619. doi:10.1073/pnas.1003600107

**Conflict of Interest:** The authors declare that the research was conducted in the absence of any commercial or financial relationships that could be construed as a potential conflict of interest.

**Publisher's Note:** All claims expressed in this article are solely those of the authors and do not necessarily represent those of their affiliated organizations, or those of the publisher, the editors, and the reviewers. Any product that may be evaluated in this article, or claim that may be made by its manufacturer, is not guaranteed or endorsed by the publisher.

Copyright © 2022 Shao, Deng, Chang, Shi, Li and Yuan. This is an open-access article distributed under the terms of the Creative Commons Attribution License (CC BY). The use, distribution or reproduction in other forums is permitted, provided the original author(s) and the copyright owner(s) are credited and that the original publication in this journal is cited, in accordance with accepted academic practice. No use, distribution or reproduction is permitted which does not comply with these terms.